

On the status of current quantum machine learning software

Manish K. Gupta ^{1[0000-0003-4226-0364]}, Tomasz Rybotycki^{1,2,3[0000-0003-2493-0459]}, and Piotr Gawron^{1,2[0000-0001-7476-9160]}

¹ Systems Research Institute Polish Academy of Sciences, ul. Newelska 6, 01-447 Warsaw, Poland

² Nicolaus Copernicus Astronomical Center, Polish Academy of Sciences, ul. Bartycka 18, 00-716 Warsaw, Poland

³ Center of Excellence in Artificial Intelligence, AGH University, al. Mickiewicza 30, 30-059 Cracow, Poland

Abstract. The recent advancements in noisy intermediate-scale quantum (NISQ) devices implementation allow us to study their application to real-life computational problems. However, hardware challenges are not the only ones that hinder our quantum computation capabilities. Software limitations are the other, less explored side of this medal. Using satellite image segmentation as a task example, we investigated how difficult it is to run a hybrid quantum-classical model on a real, publicly available quantum device. We also analyzed the costs of such endeavor and the change in quality of model.

Keywords: quantum machine learning, real devices, software

1 Introduction

Moving the frontier of quantum machine learning (QML) requires us to start performing the experiments on the real quantum devices. Only this way can we design test noise robustness of current QML algorithms and fully use the power of NISQ devices. In this work, we present a case study of using publicly available gate-based quantum computers for hyperspectral satellite image segmentation.

QML model training on a real machine is practically impossible due to the resource limitations. They can, however, be used for inference. In that case there's only one way to proceed — use classical computer to simulate the training in the environment as close to the real one, as possible. This would require us to consider the target device topology and it's noise model. We will call this approach a device-oriented training.

While the concept of device-oriented training sounds fairly simple, it's implementation requires — among others — a successful communication between different software libraries, each responsible for a specific task related to the training. During our experiments, we've noticed that this requirements isn't as straightforward as one would assume. The problem is so prominent, that we had

to resign from using one of the quantum computers available to us, due to the libraries and libraries versions incompatibility issues. Those kinds of problems are very important, although not much attention is given to them in the literature. With this paper, we aim to address this issue.

This paper is organized as follows. In section 2 we will describe our method. We introduce the hybrid quantum-classical model that we've used and it's different variations. Our focus will be particularly on the concept of the device-oriented training. We also briefly summarize our initial results in the context of the on-going research on the topic. Next, we will discuss the experiments we've done. We will start with a short description of the dataset we've used and how we planned our experiments. We will mention all the software-related issues we've encountered and assess the performance difference of our model ran using a simulator and using an actual quantum hardware. Finally, we will conclude the paper with the insights about the status of current QML software.

2 Proposed approach

For our research, we decided to tackle a problem of hyperspectral image segmentation. This is a well-known computer vision task, that draws a lot of attention, especially in the context of satellite image analysis [2]. There are two main approaches to the image segmentation. First is a pixel-level one, when each pixel is analyzed separately and a patch classification, where larger groups of neighbouring pixels are considered simultaneously [3,5]. In this work, we will focus on the first, simpler approach.

Our goal will be to detect change regions on a pair of hyperspectral images, thus we expect the output of our model to be binary, either change or no-change. Since one of our goals is to investigate the status of the QML software, we used a QML model for this task. The structure of our final model is presented in the figure 1.

To find a quantum layer with the best performance, we tried different configurations of standard embedding methods and quantum neural network (QNN) layers [6], along with the Bellman circuit layers [7] that were previously used for a similar task. The accuracies of the model we tested are presented in the table 1. Amplitude embedding and SimplifiedTwoDesign layers worked best (both separately and together), so we used them in our final model.

When we compare the results of our model with the baseline classical model from [1], we find that quantum model performs poorly in terms of classification accuracy. We'd like to point out that we didn't run the tests for the classical model — we took the results directly from [1]. The overall accuracy of our pixel-level model is about 15 percent points worse than that of the classical one. This is quite easy to explain, considering that our model had less than 200 parameters, compared to a million in the classical model. To support this claim we conducted additional experiment. We reduced the classical U-Net model [2] to a single layer of encoder and decoder. This dropped the number of trainable parameters to 1312. For a patch size of 2×2 pixels, the reduced model accuracy

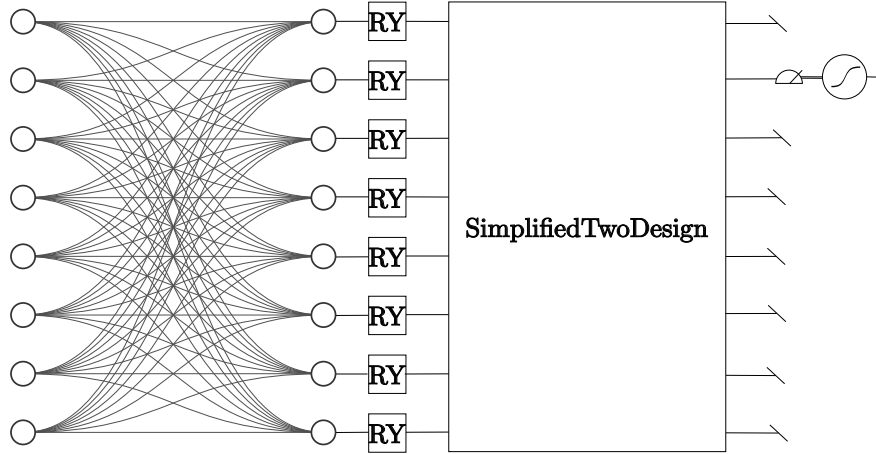


Fig. 1. A schematic of the model we used in our pixel-level change detection experiments. The input date first passes through a single layer of a classical perceptron. It is then encoded into a quantum circuit via a layer of RY gates. Then it is processed by three `SimplifiedTwoDesign` layers. We measure the expectation value of a selected qubit, pass it through a sigmoid function and return the final value as the output of the model.

Table 1. Overall accuracy of the model with respective quantum layers. Rows contain information about the embedding we used, whereas the columns describe the circuit's layers. SEL and STD denote Strongly Entangling Layer and Simplified Two Design respectively. Best accuracy scores are bolded.

	Bellman $\times 4$	SEL $\times 1$	SEL $\times 3$	STD $\times 3$
Amplitude	0.74	0.73	0.73	0.74
Angle (X)	0.52	0.66	0.73	0.73
Angle (Y)	0.52	0.67	0.71	0.74

on test dataset per class was 97.9% (change) and 25.5% (no change). The drop is significant, however, we couldn't use these results for a fair comparison, because the number of parameters in the classical network is still over 6 times higher.

2.1 Device-oriented training

To ensure the results obtained when running the model using quantum hardware are as good as possible, we wanted to train our selected model in an environment as close to the target one, as possible. This required us to select a target quantum computer, and consider it's topology, native gates and noise model during the training. In that sense, we consider this approach a device-oriented training.

We decided to divide the training into three different phases. We start with the simplest simulation, assuming interconnection between every pair of qubits and no noise. In second phase, we add the information about the device topology and the device-native gates. It's important to consider topology before the noise, because different physical qubits have different noise parameters. The noise is also typically gate-dependent and the process of circuit transpilation may significantly influence the circuit architecture. Also, noise model is usually straightforward to apply once virtual-physical qubits mapping is known and the circuit is transpiled.

For our hardware experiments, we knew we would have access to quantum computers from two different providers — IBM and IQM. Both of them use Qiskit [4] to communicate with the target device. Our main library — PennyLane [6] — can handle Qiskit, thus the transition between the hardware should be seamless. However, due to variety of issues, starting with resource access, through quantum gates implementations status between different versions of the libraries and finally due to different observable coding strategies, we couldn't run our model on the IQM device simulator. We tried using qiskit-machine-learning library to bypass the PennyLane-Qiskit-IQM configuration issues, but it didn't help. In the end, we were only able to consider the topology, but the native gates and noise model was inaccessible. Thus, we were forced to run our experiments on the IBM device only.

Although our device-oriented training was smoother for IBM device, we were not able to complete it. Although the toy models we tested could run forward- and backward passes using a noisy simulator, they were not able to complete a single epoch of the training. The common issue here were the out-of-memory problems, even on our computational clusters. While our model wasn't overly complicated, neither deep nor with a large number of qubits, noisy simulation deemed too much for current software. This highlights the limitations of current QML software and proves that the QML software requires more attention.

3 Experiments

In our research, we used standard QML libraries — PennyLane and Qiskit — with their plugins. During the study we encountered a number of software-related

issues, i.e.: libraries version dependencies conflicts, lack of support for device-native gates / standard layers, data batching issues, libraries integration issues, remote resources / access handling issues and finally out-of-memory errors that halted our pursue for complete device-oriented training. Many of the issues still remain unaddressed.

Considering only the target device (ibm_brisbane) topology and native quantum gates set, we managed to automatically reconfigure and train our model. In the end, we were able to run the model on the IBM quantum device. While analysing the results, we noticed a curious behavior of our model. Contrary to our expectations, the classification accuracy obtained using real device was much better than the accuracy of simulated model, here: 43% and 33% respectively. However, the latter accuracy was also significantly lower than expected after the training (72%, see table 1). We investigated this issue further and found out the reason. Running simulator-trained model on a real device, requires rebuilding of the quantum layer with the `PennyLane` device set to the target remote device. While we ensured that the model is properly saved and loaded, and that the weights of each layer of the model are set prior to the experiment, we **wrongly** assumed that the weights we set are automatically applied to the model during forward pass. **That is not the case**, the weights of `qml.TorchLayer` are set during creation of this `TorchLayer`, and unless explicitly specified, they will be set to random weights. **Ultimately, the model we ran on the real device, was the one with untrained quantum layer**. We already fixed this problem in our scripts.

After that realization, we started wondering if the results we obtained can still be useful, and the answer here is yes. First, since the ML task we consider is binary classification, we can simply flip the labels of the analyzed data points. This way we're starting with the classifier with 67% accuracy, instead of 33%. Moreover, since we fixed the random seeds at the beginning of the experiment, we can simulate the exact same untrained model we ran on the IBM machine. This allows us to compare both results and provide qualitative analysis. In what follows, we present an analysis of our results, after the data relabelling. Simulated results concern untrained model, the same one we used on the real device, unless otherwise stated.

The binary classification accuracy we obtained was 67% (67.438%) and 57% (56.694%) for the model ran on the simulator and the real device respectively. The accuracy dropped by 10 percent points (or roughly 15%). That's a significant drop, especially when we consider that the model accuracy isn't really impressive to begin with. It was, however, to be expected. The quantum layer of our model consists of 3 layers of a `SimplifiedTwoDesign` each built using several 2-qubit and single qubit gates. Increasing the number of gates in the circuit raises the computation time and thus influence of the decoherence. The decoherence brings the qubits' quantum state closer to the maximally mixed state⁴, hence the results

⁴ While that's not always true, the noise model used by IBM assumes that each gate is followed by (among others) a depolarizing channel which introduces the described effect.

of the classification are also more random (accuracy closer to 50%). We'd also like to point out, that the same qualitative conclusions could be made without the data relabelling.

We also analyzed a non-standard quantity which we will call the model sureness. It describes how sure the model was about the class assignment. The closer the model output was to 0.5 (the output range is [0, 1]), the less sure about the assignment it was. Formally we denote model sureness as:

$$\text{Sureness}(M) = 2 \cdot \sum_{s \in S} \frac{|M(s) - 0.5|}{|S|},$$

where S denotes the samples set, M is the model for which Sureness is computed, and $|\cdot|$ denotes either absolute value (for scalars) or power of the set. The factor 2 is used to set the sureness values range to [0, 1]. We obtained the following values:

$$\text{Sureness}(M_{\text{sim}}) = 0.118$$

$$\text{Sureness}(M_{\text{ibm}}) = 0.298$$

This result was not expected. We anticipated that the decoherence occurring on real device would bring the model closer to a random classifier, thus the model output closer to 0.5. This seems not to be the case. This result could hint at some kind of inertia-like or damping / relaxation effect occurring on IBM devices. However, further research would be required to support this hypothesis.

Alternatively, we can also look at an non-standard metric we will call confidence. It's a measure that aggregates information from the sureness and accuracy metrics. Intuitively, it describes how confident we can be in the model prediction. We assess not only if the model was correct or wrong, but also how confident it was about it. Formally we can denote the confidence as follows:

$$\text{Confidence}(M, L, S) = 1 - \sum_{i=1}^N \frac{|l_i - M(s_i)|}{N},$$

where $N := |S|$, L is the set of labels with values either 0 or 1 and the rest of the symbols is the same. We can see that the confidence is 0, when the model is always wrong and maximally sure of its decision, and 1 when it's maximally sure, but always rightfully so. We obtained the following confidence scores:

$$\text{Confidence}(M_{\text{sim}}, L, S) = 0.523 \pm 0.064$$

$$\text{Confidence}(M_{\text{ibm}}, L, S) = 0.510 \pm 0.181$$

Several conclusions follow from these results. First we can see that there's a drop in the model confidence. This is surely related to the accuracy drop between the model ran on the simulator and the real device. However, in the light of significant

Sureness increase between the same two models, it would seem that something more is going on.

To investigate this issue further, we looked upon the class prediction imbalance. What we will call imbalance is an integer value from the $[-\infty, \infty]$ interval⁵ that is the difference of the correct predictions of class 0 and class 1 by the model. Formally we can denote it as

$$\text{Imbalance}(M, L, S) = n_0(M, L, S) - n_1(M, L, S),$$

where n_i is the number of samples from S with the label i classified correctly by the model M . The greater the imbalance's absolute value, the greater was model tendency to correctly assign only one of the labels. The sign of the imbalance shows which class was classified more (less) often. The results we obtained are as follows⁶.

$$\text{Imbalance}(M_{\text{sim}}, L, S) = -110$$

$$\text{Imbalance}(M_{\text{ibm}}, L, S) = -647$$

The results show that both models had a tendency to guess class 1 better, but for a model ran on the real device, this tendency was significantly higher. An important thing to note here is the fact that we did the relabelling before the analysis. This means that class 1 predictions are made when the output of the model is low, that is the $|1\rangle$ state counts were low. Imbalance analysis led us to believe that we're experiencing a significant influence of the relaxation-type decoherence on the real device. This hypothesis is further supported by the observation that Qiskit devices' error model is constructed using thermal relaxation error channels. However, further research in this area would be needed to support this claim.

Our code and the data we gathered are available on Gitlab [8] and Zenodo [9], respectively.

4 Conclusions

The conclusion we draw from these experiments is that the available software frameworks, i.e. PennyLane and Qiskit, do not fully support noisy simulation of quantum machine learning models. They not only over-complicate the process by hiding the physical-virtual qubit correspondence, but also cannot support the simulations due to computational complexity. In case of PennyLane, even the noise model itself is not complete (it lacks readout errors). To some limited extent, however, it seems possible to at least run the noisy forward pass for single samples.

⁵ With the information about the shots number, the imbalance can be normalized.

⁶ For simulated model we obtained $n_0 = 557$ and $n_1 = 667$. For model ran on the IBM device we got $n_0 = 192$ and $n_1 = 839$. Remember that the classes were relabelled!

These libraries are also subject to technical errors, which have to be either corrected manually or submitted as an issue to their respective developers. In both cases, the process is time-consuming and reduces the usability and confidence we can have in those libraries. This highlights the need for a discussion on a status of the current QML software.

Our results also suggest that the QML models ran on real devices are highly unreliable and inaccurate. The cause of this behavior is undoubtedly the noise occurring during data processing on real devices. We believe that current quantum devices are not ready for running complex ML models. Especially one trained in a noiseless environment.

Acknowledgment

Supported by ESA under the contract No. 4000137375/22/NL/GLC/my. Supported by PMW programme under the contract No. 5304/ESA/2023/0. The simulations were carried out based on the IBM Quantum environment, access to which is financed within the framework of the project “Development of digital competences in quantum engineering in 2024-2025” carried out by the Poznan Supercomputing and Networking Center. PG and TR gratefully acknowledge the funding support by program “Excellence initiative—research university” for the AGH University in Krakow as well as the ARTIQ project: UMO-2021/01/2/ST6/00004 and ARTIQ/0004/2021.

References

1. R. Caye Daudt, B. Le Saux, A. Boulch, and Y. Gousseau. Urban change detection for multispectral earth observation using convolutional neural networks. In *IEEE International Geoscience and Remote Sensing Symposium (IGARSS)*, July 2018.
2. Rodrigo Caye Daudt, Bertr Le Saux, and Alexandre Boulch. Fully convolutional siamese networks for change detection. In *2018 25th IEEE International Conference on Image Processing (ICIP)*, pages 4063–4067, 2018.
3. Iris Cong, Soonwon Choi, and Mikhail D. Lukin. Quantum convolutional neural networks. *Nature Physics*, 15(12):1273–1278, 2019.
4. Ali Javadi-Abhari, Matthew Treinish, Kevin Krsulich, Christopher J. Wood, Jake Lishman, Julien Gacon, Simon Martiel, Paul D. Nation, Lev S. Bishop, Andrew W. Cross, Blake R. Johnson, and Jay M. Gambetta. Quantum computing with Qiskit, 2024.
5. Seunghyeok Oh, Jaeho Choi, and Joongheon Kim. A tutorial on quantum convolutional neural networks (qcnn), 2020.
6. PennyLane Development Team. *PennyLane Documentation Guide*, 2025. Accessed online: <https://docs.pennylane.ai/en/stable/development/guide/documentation.html>.
7. Alessandro Sebastianelli, Daniela Alessandra Zaidenberg, Dario Spiller, Bertrand Le Saux, and Silvia Liberata Ullo. On circuit-based hybrid quantum neural networks for remote sensing imagery classification. *IEEE Journal of Selected Topics in Applied Earth Observations and Remote Sensing*, 15:565–580, 2022.

8. SIPwQNN Team. qnn_change_detection: Sipwqnn repository. https://github.com/Tomev/qnn_change_detection, 2025. GitHub repository.
9. SIPwQNN Team. Spectral Information Processing with Quantum Neural Networks samples from ibm_brisbane. <https://zenodo.org/uploads/14784888>, 2025. Zenodo page with the samples we collected.